Environmental Research Letters

Mortality tradeoff between air quality and skin cancer from changes in stratospheric ozone

Environmental Research Letters

LETTER

Mortality tradeoff between air quality and skin cancer from changes in stratospheric ozone

Sebastian D Eastham[1,3], David W Keith[2] and Steven R H Barrett[1]

[1] Laboratory for Aviation and the Environment, Massachusetts Institute of Technology, 77 Massachusetts Avenue, Cambridge, MA 02139, United States of America
[2] School of Engineering and Applied Sciences, Harvard University, Cambridge, MA 02138, United States of America
[3] Author to whom any correspondence should be addressed.

E-mail: seastham@mit.edu

OPEN ACCESS

RECEIVED
3 December 2017

REVISED
12 January 2018

ACCEPTED FOR PUBLICATION
6 February 2018

PUBLISHED
9 March 2018

Keywords: stratospheric ozone, air quality, UV-B, skin cancer, public health

Abstract

Skin cancer mortality resulting from stratospheric ozone depletion has been widely studied. Similarly, there is a deep body of literature on surface ozone and its health impacts, with modeling and observational studies demonstrating that surface ozone concentrations can be increased when stratospheric air mixes to the Earth's surface. We offer the first quantitative estimate of the trade-off between these two effects, comparing surface air quality benefits and UV-related harms from stratospheric ozone depletion. Applying an idealized ozone loss term in the stratosphere of a chemistry-transport model for modern-day conditions, we find that each Dobson unit of stratospheric ozone depletion results in a net decrease in the global annual mortality rate of ~40 premature deaths per billion population (d/bn/DU). The impacts are spatially heterogeneous in sign and magnitude, composed of a reduction in premature mortality rate due to ozone exposure of ~80 d/bn/DU concentrated in Southeast Asia, and an increase in skin cancer mortality rate of ~40 d/bn/DU, mostly in Western Europe. This is the first study to quantify air quality benefits of stratospheric ozone depletion, and the first to find that marginal decreases in stratospheric ozone around modern-day values could result in a net reduction in global mortality due to competing health impact pathways. This result, which is subject to significant methodological uncertainty, highlights the need to understand the health and environmental trade-offs involved in policy decisions regarding anthropogenic influences on ozone chemistry over the 21st century.

Introduction

The Montreal protocol averted a potentially catastrophic loss of stratospheric ozone by restricting emissions of ozone-depleting substances (Slaper *et al* 1996, van Dijk *et al* 2013). With the gradual recovery of the ozone layer now underway, it is important to consider how the ozone layer will further evolve in response to changing anthropogenic drivers, including the falling stratospheric chlorofluorocarbon burden, climate change, aircraft emissions, and potentially solar geoengineering (Pitari *et al* 2015, Tilmes *et al* 2012, Keith *et al* 2016). Some combinations of anthropogenic forcing may even drive stratospheric ozone concentrations beyond pre-industrial levels, a so-called 'super-recovery' (Li *et al* 2009). Previous risk assessments of changes in stratospheric ozone have focused on UV flux, but stratospheric ozone is also transported to the surface (Lin *et al* 2012, 2015, Hsu and Prather 2009), increasing surface ozone concentrations and posing health risks. This implies that a decrease in stratospheric ozone concentrations may reduce respiratory disease mortality, providing a benefit which can be compared against the cost of increasing mortality from skin cancer.

The health and environmental tradeoffs associated with changes in stratospheric ozone must be assessed if informed policy choices are to be made regarding these drivers. We use the GEOS-Chem unified stratospheric-tropospheric global chemical transport model to quantify the sensitivity of surface ozone and incident UV-B radiation to changes in stratospheric

ozone. We then estimate the associated change in mortality rates using epidemiological exposure response functions, applied to spatially-resolved estimates of current mortality rates (Slaper *et al* 1996, Jerrett *et al* 2009). We quantify premature mortality impacts resulting from changes in exposure to surface-level ozone (i.e. respiratory disease) and UV radiation (skin cancer) following a marginal decrease in stratospheric ozone. Other effects, such as changes in non-fatal skin cancer incidence rates, crop damage, and loss of vegetation, are not considered. Previous work has quantified impacts of increased exposure to UV radiation due to ozone depletion (Slaper *et al* 1996, van Dijk *et al* 2013), but to date there has been no quantitative estimate of benefits associated with reduced exposure to surface-level ozone. This is the first study to directly compare UV-related damages to air quality benefits, both of which must be considered for a balanced understanding of the consequences.

Materials and methods

We use v11-01 of the GEOS-Chem global chemistry-transport model to estimate the effect of marginal stratospheric ozone depletion on atmospheric composition and intensity of UV-B radiation at the surface. All simulations are conducted at a horizontal resolution of $4° \times 5°$, with a dynamic time step of 30 minutes and chemical time step of 60 minutes. GEOS-Chem uses a fully interactive troposphere and stratosphere, applying a unified chemistry mechanism from the surface to the stratopause (Eastham *et al* 2014). UV intensity is calculated from the output of the 18-bin high-frequency radiative transfer model embedded in the Fast-JX 7.0a photolysis code used by GEOS-Chem.

Meteorological data is read from the MERRA-2 long-term reanalysis dataset, and all simulations are performed at MERRA-2's native, 72-layer vertical resolution, using identical emissions data. We use the EDGAR v4.2 inventory for global anthropogenic emissions (JRC and PBL 2014), although biomass burning emissions are calculated based on GFED-4 (Giglio *et al* 2013) and regional inventories are used in place of EDGAR where available. These include the 2005 EMEP inventory for Europe, the 2011 National Emissions Inventory for the US, the 2005 Criteria Air Contaminants inventory for Canada and the 2010 MIX inventory for Asia. Aircraft emissions are calculated using the MIT Aircraft Emissions Inventory Code (AEIC) for 2005 (Simone *et al* 2013). Lightning NO_x emissions are calculated based on Murray *et al* (2012).

The model is initially spun up without any additional ozone loss terms for four simulation years, using data for January 2011–December 2014. Three independent simulations are then initialized using the final model state. The first is the baseline simulation, BASE, in which no additional ozone loss terms are applied. The second simulation, ALL, includes a uniform, artificial ozone loss term applied between the tropopause and a pressure-altitude of 10 hPa (~30 km). The final simulation, LOWER, reduces the upper boundary of this range to 150 hPa (~14 km). If the tropopause exceeds this altitude in a given location, then this loss term is not applied. Each of these three simulations is spun up for a further four years using the same 2011–2014 meteorological data, the result of which is used to initialize a third and final four-year simulation period using the same four years of meteorological data. The final year of this period is used to calculate changes in exposure relative to BASE.

The ozone loss term in the ALL and LOWER simulations is applied using GEOS-Chem's Kinetic Pre-Processor (KPP) chemistry solver as a first-order chemical loss term of the form

$$\mathrm{d}[O_3]/\mathrm{dt} = -k[O_3]$$

where the rate constant k is given a value of 10^{-9} s^{-1}. This value is chosen to be large enough to ensure a visible signal in the output while also being small enough to prevent large-scale ozone loss. The net change in the average global ozone column is 1.7 DU (ALL-BASE) and 0.04 DU (LOWER-BASE). To address concerns regarding response linearity, we conduct an additional follow-up simulation using a 40 times great depletion rate for the LOWER scenario. This yields a change of 1.5 DU, but the total change in mortality per DU is within 1.0% of the normalized value from the LOWER scenario.

Premature mortality impacts are calculated using the method outlined in Eastham and Barrett (2016). Surface ozone mixing ratios and incident UV radiation intensity are compared to a reference simulation of the year 2015. This is the most recent year for which comprehensive age-, country- and cause-specific mortality data are available from the World Health Organization (WHO 2016). Population distribution data is taken from the 2012 LandScan estimate on a $0.083° \times 0.083°$ grid, and scaled to 2015 using data from the UN Population Prospects division (UN 2013). Surface and UV intensity and ozone mixing ratio data from each simulation are regridded, without interpolation, onto the finer $0.083° \times 0.083°$ grid.

Ozone-related mortality rates in each cell are calculated using a log-linear exposure response function of the form

$$\Delta I = I_B \left(\mathrm{RR}_R^{\left(\frac{\Delta X}{\Delta X_R}\right)} - 1 \right)$$

where I_B is the baseline incidence rate of the given disease in mortalities per capita per year. RR_R is the reference, unitless relative risk taken from the original epidemiological study, equivalent to the relative change in mortality rate associated with the ΔX_R change in ozone mixing ratio observed in said study. ΔX is the change in ozone mixing ratio between the target and

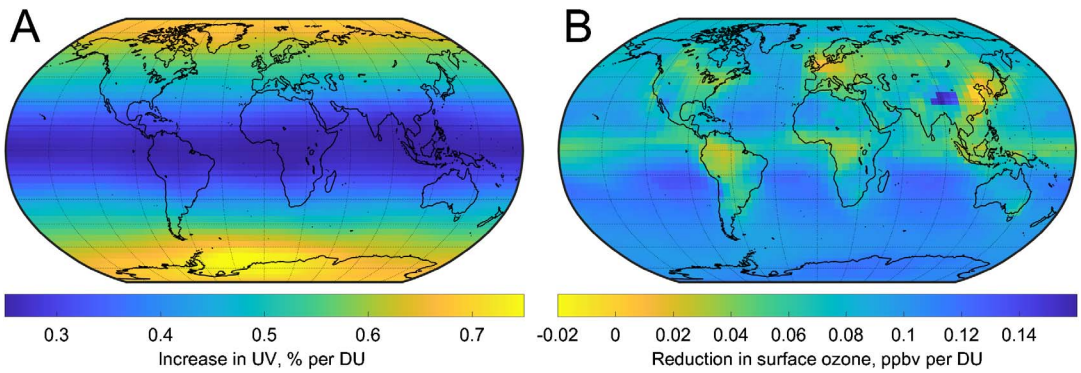

Figure 1. Increase in surface UV radiation (left) and decrease in surface ozone (right), divided by the global average reduction in stratospheric ozone in Dobson Units (DU). UV is shown in terms of the fractional change in the absolute annual average, whereas ozone changes are shown as an absolute change in the ozone-season one-hour maximum value, to reflect the different characteristics of the exposure response functions. In both cases, dark blue colors correspond to less harmful (more beneficial) outcomes of stratospheric ozone loss, while light yellow colors correspond to more harmful (less beneficial) outcomes.

reference simulation, and ΔI is the resulting change in incidence. Values of RR_R and ΔX_R for this work are taken from Jerrett *et al* (2009), in which a 10 ppbv increase in exposure results in a ~4% (95% CI: 1%–6.7%) excess risk of respiratory disease mortality. For consistency with the study, we use the one-hour maximum ozone mixing ratio averaged over the local six-month ozone season to calculate the change in exposure, and the change in incidence rate is applied to the local population of age 30 or greater only. Ozone is assumed to affect mortality due to chronic obstructive pulmonary disease and asthma.

UV-related mortality rates are calculated using a power-law exposure response function described by Slaper *et al* (1996), of the form

$$\Delta I = I_B(E/E_{2015})^C$$

where E is the intensity of UV-radiation under the given scenario, E_{2015} is the intensity under the 2015 reference scenario, and C is a disease-specific power factor. Simulated UV radiation intensity is weighted according to the SCUP-h action spectrum (de Gruijl *et al* 1994). We use a value of 0.6 (95% CI: 0.2–1.0) for C. We consider only cutaneous melanoma mortality, and do not correct for possible underreporting.

Each mortality calculation is performed three times using the lower 95% bound, central estimate, and upper 95% bound of the estimated exposure response function slope. Total mortality is estimated by assuming that each follows a triangular distribution with the same 95% intervals and taking the central estimate as the modal value. A Monte-Carlo simulation is then performed using 10^8 independent samples to estimate the median value and the 2.5th and 97.5th percentiles.

Results and discussion

We simulate stratospheric ozone depletion by applying a uniform loss factor of 10^{-9} s^{-1} from the tropopause to a pressure-altitude of 10 hPa (~30 km). Because of the net export of ozone from the tropics, a uniform ozone depletion rate results in greater accumulated column loss at high latitudes than at low latitudes, and therefore in a greater fractional increase in surface UV intensity. Figure 1(*a*) shows the percent increase in surface UV radiation per unit decrease in global mean column ozone. Per Dobson unit (DU) of global average column ozone loss, surface UV intensity over populated areas increases by between 0.25% at the equator and 0.65% at high latitudes. For context, the ozone super-recovery has been projected to result in increased global average column ozone of ~10 DU, while the most recent report from the World Meteorological Organization shows a 20 DU decrease in the total ozone column (60° S–60° N) between 1960 and 2000, due largely to ozone depleting substances (Li *et al* 2009, WMO 2014).

The decrease in stratospheric ozone abundance also drives a reduction in surface ozone concentrations. The magnitude of this effect varies with location, as shown in figure 1(*b*), and is made up of two factors. Reduced stratospheric ozone abundance means that stratospheric air which crosses the tropopause and descends towards the surface contains a proportionally reduced concentration of ozone (Hsu and Prather 2009). Increased UV intensity also results in faster rates of both production and destruction of tropospheric ozone, and therefore a decrease in ozone lifetime (Zhang *et al* 2014). The combined result is that stratospheric ozone loss results in surface ozone concentrations being reduced in almost all locations, falling by between 0 and 0.15 ppbv per DU. These surface ozone reductions are maximized in regions which frequently observe stratospheric intrusions, such as the Western coast of the USA and the Tibetan Plateau (Lin *et al* 2012, 2015). The only observed increase in surface ozone is on the Eastern coast of China. This reversal in the sign of the sensitivity may be due to the highly polluted conditions in this region, as increased UV fluxes in regions of very high NO_x can result in additional ozone production through NO_x cycling (Liu and Trainer 1988).

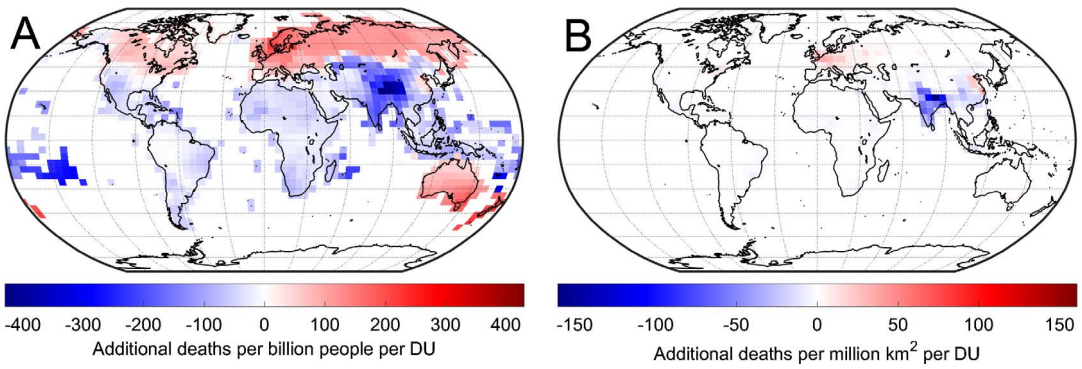

Figure 2. Global sensitivity of annual premature mortality rate to stratospheric ozone loss, including both skin cancer and respiratory disease. Figure 2(*a*) shows premature mortality rates per billion people per DU reduction in global average ozone column (d/bn/DU), and 2B shows premature mortalities per unit area per DU (d/km^2/DU). Positive values correspond to increases in overall premature mortality risk in response to stratospheric ozone depletion.

Figure 2 shows the estimated change in premature mortality associated with stratospheric ozone depletion, per unit global average reduction in ozone column. The number of premature mortalities is divided by the local population (2A) and by area (2B). We find that stratospheric ozone destruction results in 41 fewer premature mortalities per year per billion people per Dobson unit (d/bn/DU) (95% confidence interval of −25 to 100 fewer d/bn/DU). This total is made up of 83 fewer d/bn/DU due to respiratory disease (95% CI: 21–140), and 39 additional d/bn/DU per year due to skin cancer (95% CI: 13–66). These estimates only include uncertainty in the exposure response functions, and not in atmospheric modeling.

The calculated increases in skin cancer mortality rates are greatest at high latitudes due to the greater increase in UV exposure and the higher baseline rates of melanoma mortality. The greatest change in skin cancer mortality rate occurs in New Zealand, with an additional 340 d/DU/bn (110–580). However, figure 2(*b*) demonstrates that the largest absolute increases in total premature mortalities occur in the Northern mid-latitudes due to higher population densities and greater susceptibility to skin cancer. 53% of the total increase occurs in seven countries. China, the USA and Russia experience 15%, 14% and 8% respectively, while Germany, the UK, France and Italy combined contribute a further 15%.

By contrast, the reduction in mortality resulting from reduced exposure to ozone of stratospheric origin is maximized in South Asia. The impact of the physical changes shown in figure 1 is again moderated by variations in population density and baseline mortality rates. For example, the data used in this study reports a 2015 mortality rate due to respiratory diseases of 170 deaths per 100 000 people of age 30+ in India, compared to 91 deaths per 100 000 in the same age group for the USA. These factors combine to produce a peak in the absolute change in mortality around India (figure 2(*b*)), such that prevented mortalities in India and China contribute 38% and 13% of the total benefit, respectively.

Considering only mortality impacts from skin cancer and respiratory disease, and subject to uncertainty in models of exposure response and atmospheric chemistry, small reductions in stratospheric ozone around current levels result in a marginal net decrease in global premature mortality. The net global decrease of 41 d/bn/DU is made up of competing changes which are up to ten times greater in magnitude, with health benefits in Asia exceeding disbenefits in Europe and Australasia.

Relevant to the lower stratospheric loss mechanisms in which halogens and sulfate aerosols play a dominant role (Tilmes *et al* 2012), we conduct an additional experiment in which the ozone loss term is restricted to the lowermost stratosphere. This biases depletion towards lower altitudes, increasing the relative impact on surface ozone mixing ratios and redistributing stratospheric ozone loss towards the poles and away from population centers (figure 3). This alternate loss term results in a global reduction in mortality rate of 260 d/bn/DU (95% CI: 33–480), compared to 41 d/bn/DU (–39 to 83) when depletion continues up to 10 hPa. This implies that the net change in mortality will depend on the specific pattern of ozone depletion, which will vary between different anthropogenic drivers. Midlatitude ozone depletion from CFCs, which is greatest in the upper stratosphere, will provide less benefit in terms of respiratory mortality for each DU lost than depletion occurring in the lower stratosphere, while providing a similar increase in skin cancer mortality.

These mortality sensitivity calculations are subject to significant uncertainty. Uncertainty in the exposure response function is partially quantified in the reported 95% confidence intervals, but there remain other, potentially large sources of uncertainty which are not quantified. The given intervals do not account for uncertainty in the shape or functional form of the exposure response. Although recent work has

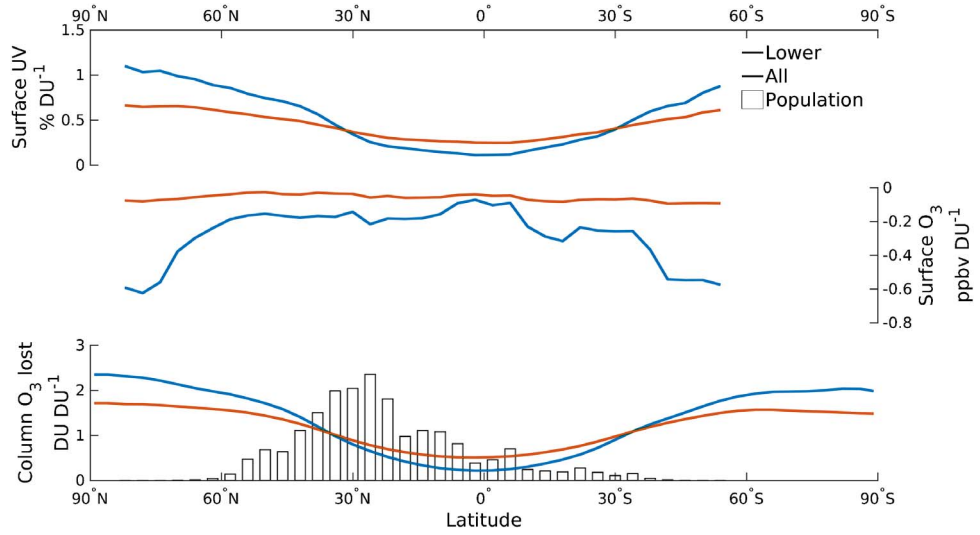

Figure 3. Changes in ozone column, surface ozone and surface exposure to UV radiation, divided by the global average reduction in column ozone for two different depletion scenarios. Surface quantities are weighted by population density within each latitude band. The fraction of global population within each latitude is shown as empty black bars. Change in UV is calculated as the increase in UV exposure divided by exposure in an unperturbed simulation for 2015, the year for which the WHO mortality data was collected. All data is divided by the global mean change in ozone column depth, such that the local column ozone lost per unit of global column ozone loss in the final panel averages to 1.0 for both scenarios.

suggested that the impacts of short-term exposure to ozone are unlikely to have a lower concentration threshold (Di *et al* 2017), the validity of this assumption is not yet known for long-term exposure. The same arguments are true for exposure to UV radiation. We also do not account for possible under-reporting of melanoma mortality in less-developed regions, which will result in an underestimate of mortality changes due to increased UV radiation (van Dijk *et al* 2013). Non-mortality impacts associated with both UV and ozone exposure are not quantified. In the case of UV radiation, these include both benefits and costs associated with increased exposure, and the sign of the response is uncertain. For ozone, reduced exposure is expected to decrease hospital admission rates (European Commission 2005), and reduced tropospheric ozone mixing ratios could suppress formation of harmful particulate matter (Eastham and Barrett 2016). Furthermore, we do not account for impacts due to changes in acute exposure. This would increase the impact of changes in surface ozone, but the disproportionately greater reduction in upper tropospheric ozone could also incur benefits due to reductions in acute ozone exposure for airline passengers.

Modeling uncertainties in atmospheric transport and chemistry are also not quantified. All simulations are performed using a grid resolution of 4° × 5°. Simulations at this resolution are able to capture large scale or diffuse features such as the proportional change in downwelling ozone and UV-B radiation. Fine grid resolution is also not inherently necessary to capture spatial information relevant to ozone-induced health impacts, as mortality impacts of ozone have been found to be well-represented in coarse-resolution data (Punger and West 2013). However small scale dynamical features such as tropopause folds are less well resolved, and localized features such as urban pollution are artificially diluted. As such, changes in surface ozone due to non-linear, UV-sensitive plume chemistry are likely to be underestimated. An investigation using a high-resolution global model is an area for future research. Recalculation of mortality using data from other simulation years resulted in changes of up to 7% for additional skin cancer mortality, and of up to 30% for prevented respiratory disease mortalities. For all years simulated, the ratio of prevented respiratory mortality to induced skin cancer mortality was greater than or equal to the 2015 value.

Conclusions

Marginal stratospheric ozone depletion is found to provide reductions in respiratory disease mortalities of similar or greater magnitude than the associated increase in skin cancer mortality. Although the sign of the net change is uncertain due to the competition between changes in UV exposure and air quality, the central estimate is of a net benefit. The relative magnitude and net sign of these tradeoffs vary as a function of geographic location but also as a function of the spatial and temporal distribution of the change in stratospheric ozone abundance. 21st century stratospheric ozone changes will be driven by factors including: decreasing stratospheric CFC loading, increasing NO_x from aviation and N_2O, and potentially some form of solar geoengineering that might decrease or increase ozone loss rates (Tilmes *et al* 2012, Keith *et al* 2016, IPCC 2014). Changes in stratospheric water vapor and temperature due to anthropogenic

climate change may even drive an ozone super-recovery, which this work suggests would result in a net increase in global mortality. Each of these drivers will result in a different seasonality and distribution of changes in stratospheric ozone, in turn altering the magnitude, sign and distribution of impacts on human health, agriculture, and the environment. For a given change in global column ozone, and considering only premature mortalities, processes that reduce lower stratospheric ozone will cause less harm and provide greater benefits than those which produce the same change in column ozone by reducing upper stratospheric ozone. Further research is needed to reduce these uncertainties and better inform decisions about management of anthropogenic emissions that impact stratospheric ozone chemistry.

Acknowledgments

The MERRA-2 data used in this study have been provided by the Global Modeling and Assimilation Office (GMAO) at NASA Goddard Space Flight Center. We would also like to thank Loretta Mickley for discussions regarding the relative role of transport and photochemistry.

ORCID iDs

Sebastian D Eastham https://orcid.org/0000-0002-2476-4801

References

de Gruijl F R and Van der cLeun J C 1994 Estimate of the wavelength dependency of ultraviolet carcinogenesis in humans and its relevance to the risk assessment of a stratospheric ozone depletion *Health Phys.* **67** 319–25

Di Q, Dai L, Wang Y, Zanobetti A, Choirat C, Schwartz J D and Dominici F 2017 Association of short-term exposure to air pollution with mortality in older adults *JAMA* **318** 2446–56

Eastham S D, Weisenstein D K and Barrett S R H 2014 Development and evaluation of the unified tropospheric–stratospheric chemistry extension (UCX) for the global chemistry-transport model GEOS-Chem *Atmos. Environ.* **89** 52–63

Eastham S D and Barrett S R H 2016 Aviation-attributable ozone as a driver for changes in mortality related to air quality and skin cancer *Atmos. Environ.* **144** 17–23

European Commission 2005 ExternE—Externalities of Energy: Methodology 2005 Update

Giglio L, Randerson J T and van der Werf G R 2013 Analysis of daily, monthly, and annual burned area using the fourth-generation global fire emissions database (GFED4) *J. Geophys. Res. Biogeosci.* **118** 317–28

Hsu J and Prather M J 2009 Stratospheric variability and tropospheric ozone *J. Geophys. Res.* **114** D06102

Intergovernmental Panel on Climate Change (IPCC) 2014 Summary for policymakers *Climate Change 2014: Impacts, Adaptation, and Vulnerability. Part A: Global and Sectoral Aspects. Contribution of Working Group II to the Fifth Assessment Report of the Intergovernmental Panel on Climate Change* ed C B Field *et al* (Cambridge: Cambridge University Press) pp 1–32

Jerrett M *et al* 2009 Long-term ozone exposure and mortality *N. Engl. J. Med* **360** 1085–95

JRC (European Commission Joint Research Center) and PBL (Netherlands Environmental Assessment Agency) 2014 Emission Database for Global Atmospheric Research (EDGAR), release EDGARv4.2 FT2012

Keith D W, Weisenstein D K, Dykema J A and Keutsch F N 2016 Stratospheric solar geoengineering without ozone loss *Proc. Natl Acad. Sci. USA* **113** 14910–4

Li F, Stolarski R S and Newman P A 2009 Stratospheric ozone in the post-CFC era *Atmos. Chem. Phys.* **9** 2207–13

Lin M *et al* 2012 Springtime high surface ozone events over the western United States: quantifying the role of stratospheric intrusions *J. Geophys. Res* **117** D00V22

Lin M *et al* 2015 Climate variability modulates western US ozone air quality in spring via deep stratospheric intrusions *Nat. Commun.* **6** 7105

Liu S C and Trainer M 1988 Responses of the tropospheric ozone and odd hydrogen radicals to column ozone change *J. Atmos. Chem.* **6** 221–33

Murray L T, Jacob D J, Logan J A, Hudman R C and Koshak W J 2012 Optimized regional and interannual variability of lightning in a global chemical transport model constrained by LIS/OTD satellite data *J. Geophys. Res.* **117** D20307

Pitari G *et al* 2015 Impact of coupled NO_x/Aerosol aircraft emissions on ozone photochemistry and radiative forcing *Atmosphere* **6** 751–82

Punger E M and West J J 2013 The effect of grid resolution on estimates of the burden of ozone and fine particulate matter on premature mortality in the USA *Air Qual. Atmos. Health* **6** 563

Simone N W, Stettler M E J and Barrett S R H 2013 Rapid estimation of global civil aviation emissions with uncertainty quantification *Transp. Res. Part D: Trans. Environ.* **25** 33–41

Slaper H, Velders G J, Daniel J S, de Gruijl F R and van der Leun J C 1996 Estimates of ozone depletion and skin cancer incidence to examine the Vienna convention achievements *Nature* **384** 256–8

Tilmes S *et al* 2012 Impact of very short-lived halogens on stratospheric ozone abundance and UV radiation in a geo-engineered atmosphere *Atmos. Chem. Phys.* **12** 10945–55

United Nations Department of Economic and Social Affairs (Population Division) 2013 World Population Prospects: The 2012 revision

van Dijk A *et al* 2013 Skin cancer risks avoided by the Montreal Protocol–worldwide modeling integrating coupled climate-chemistry models with a risk model for UV *Photochem. Photobiol.* **89** 234–46

World Health Organization 2016 *Global Health Estimates 2015: Deaths by Cause, Age, Sex, by Country and by Region* pp 2000–15

World Meteorological Organization 2014 *Update on Global Ozone: Past, Present, and Future Scientific Assessment of Ozone Depletion: 2014 Global Ozone Research and Monitoring Project—Report 55* (Geneva: World Meteorological Organization)

Zhang H, Wu S, Huang Y and Wang Y 2014 Effects of stratospheric ozone recovery on photochemistry and ozone air quality in the troposphere *Atmos. Chem. Phys.* **14** 4079–86